

Filtering Technique to Control Member Size in Topology Design Optimization

Tae Soo Kim, Jae Eun Kim, Je Hyun Jeong, Yoon Young Kim*

School of Mechanical and Aerospace Engineering, Seoul National University,
Shinlim-Dong, San 56-1, Kwanak-Gu, Seoul 151-742, Korea

A simple and effective filtering method to control the member size of an optimized structure is proposed for topology optimization. In the present approach, the original objective sensitivities are replaced with their relative values evaluated within a filtering area. By adjusting the size of the filtering area, the member size of an optimized structure or the level of its topological complexity can be controlled even within a given finite element mesh. In contrast to the checkerboard-free filter, the present filter focuses on high-frequency components of the sensitivities. Since the present filtering method does not add a penalty term to the objective function nor require additional constraints, it is not only efficient but also simple to implement. Mean compliance minimization and eigenfrequency maximization problems are considered to verify the effectiveness of the present approach.

Key Words : Member Size, Topology Optimization, Filter, Design Sensitivity

1. Introduction

The main objective of topology optimization is to improve the structural performance such as mean compliance and eigenfrequencies. However, some issues such as manufacturability and aesthetics cannot be overlooked. Unfortunately, these issues are difficult to impose in the form of either an objective function or a side constraint. The motivation of this investigation is to develop an effective member-size controlling method to meet designers' need to address the manufacturability and aesthetics issues.

When structures are subjected to repeated loads, designs having simply topological connectivity with large member sizes are usually preferred. For example, some methods such as the multiresolution strategy (Kim and Yoon, 2000)

can be employed to achieve this goal. On the other hand, there appears no work yet reported to control the maximum size of each of the structural members. This member-size controlling issue can be quite significant especially when manufacturability and aesthetics are to be addressed. To control the member size, a perimeter-controlling method (Haber et al., 1996) or a density-slope constraining method (Petersson and Sigmund, 1998; Zhou et al., 2001) may be employed, but these methods are difficult to make the member sizes of an optimized design smaller than a certain value. In this work, we propose a simple but powerful filtering method to control the member size of an optimized structure.

Filtering methods (Sigmund, 1994; Park and Yoon, 1997; Yoon and Park, 1997) were introduced earlier to suppress the unwanted formation of checkerboard patterns. In topology optimization, two filters, a checkerboard-free filter and a mesh-independence filter, are currently widely used. Mathematical discussions on these filters may be found in Bourdin (2001). The filters modify the original sensitivities of an objective function by passing low-frequency components of

* Corresponding Author,

E-mail : yykim@snu.ac.kr

TEL : +82-2-880-7154; FAX : +82-2-883-1513

School of Mechanical and Aerospace Engineering,
Seoul National University, Shinlim-Dong, San 56-1,
Kwanak-Gu, Seoul 151-742, Korea. (Manuscript Received July 18, 2003; Revised October 25, 2003)

them. Therefore, the application of these filters reduces the topology complexity of an optimized structure.

The filter which we propose for member-size control is similar to the checkerboard-free and the mesh-independence filters in which it also modifies the original sensitivities of an objective function. However, we focus on the high-frequency components of the sensitivity field in order to decrease the size of each member of an optimized structure. To this end, the original sensitivities are replaced with the relative sensitivities that are reevaluated within a given member-size filtering area. The corresponding filter will be called the member-sizing filter. As the area of the member-sizing filter becomes smaller, the member size becomes smaller and a more complex topological configuration is obtained even in a fixed finite element mesh. We use four-node plane finite elements for the analysis, and thus we use the checkerboard-free filter before applying the present member-sizing filter.

As an optimizer, we use the optimality criteria method in updating design variables. In the vibration-related problems, however, the optimality criteria should be modified since the signs of design sensitivities may be either positive or negative. In order to apply the proposed filter, we also modify the optimality criteria by extending the idea of Ma et al. (1993).

Since the member-sizing filter modifies the original sensitivity field, the functional performance of the resulting design may be somewhat deteriorated. Considering the manufacturability and aesthetics aspects of the final optimized design, however, this may be endured.

2. Various Schemes to Control Shape and Topology of an Optimized Structure

A structural topology optimization problem (Bendsøe and Sigmund, 2003) in finite element formulation can be stated as

$$\text{Minimize } f(\boldsymbol{\rho}) \quad (1)$$

$$\text{subject to } g(\boldsymbol{\rho}) = \sum_{i=1}^{N_e} \rho_i v_i - M_0 = 0 \quad (2)$$

$$0 < \rho_i \leq 1, \quad i=1, 2, \dots, N_e \quad (3)$$

where ρ_i is the design variable associated with the i th finite element, and N_e is the number of design variables. The symbol v_i is the volume of the i th finite element, and M_0 is the prescribed mass. For mean compliance minimization and multiple eigenfrequency maximization problems, the corresponding objective function f can be expressed as respectively.

$$f(\boldsymbol{\rho}) = \mathbf{f}^T \mathbf{u} \quad (4)$$

$$f(\boldsymbol{\rho}) = -\ln(\lambda_1^{w_1} \lambda_2^{w_2} \dots \lambda_{N_\lambda}^{w_{N_\lambda}}) \quad (5)$$

In Eq. (4), the force vector \mathbf{f} and the displacement vector \mathbf{u} are related by the stiffness matrix \mathbf{K} as $\mathbf{K}\mathbf{u}=\mathbf{f}$. The eigenvalue λ_j in Eq. (5) is the solution of the following equation

$$\mathbf{K}\mathbf{u}_j = \lambda_j \mathbf{M}\mathbf{u}_j \quad (6)$$

where \mathbf{M} is the mass matrix and w_j ($j=1, \dots, N_\lambda$) are weighting factors. The advantage of using the objective function in the form of Eq. (5) may be found in Ma et al. (1995) and Kim and Kim (2002).

Using the SIMP (Solid Isotropic Material with Penalization) approach, the i th element stiffness and element mass matrix are written as

$$\mathbf{K}_i = \rho_i^n \mathbf{K}_i^0 \quad (7)$$

$$\mathbf{M}_i = \rho_i \mathbf{M}_i^0 \quad (8)$$

where \mathbf{K}_i^0 and \mathbf{M}_i^0 are the matrices for $\rho_i=1$, and n is the penalization factor (throughout all numerical examples, n of 2.5 is used).

In solving optimization problems described above, various schemes have been proposed to control the shape and topology of an optimized structure. In what follows, a brief review of existing methods is given.

2.1 Perimeter-control

The perimeter-control method along with its numerical implementation was given by Haber et al. (1996). They defined a quantity that measures

the boundary perimeter of a discretized structure as

$$P = \sum_{k=1}^K l_k (\sqrt{\langle \rho \rangle_k^2 + \varepsilon^2} - \varepsilon) \quad (9)$$

$$S = P_0 \ln |P_0 - P| \quad (10)$$

In Eq. (9), $\langle \rho \rangle_k$ is the difference in the design variables along the interface of the k th finite element having length l_k and K is the number of finite element interfaces. A small positive number ε is introduced to guarantee the differentiability of the perimeter with respect to the design variables.

The perimeter of an optimized structure is enforced by adding a penalty function S in Eq. (10) to the objective function. Since it is difficult to define the desired value P_0 of the perimeter of an optimized structure in advance, several numerical experiments may be needed. With a properly selected perimeter value P_0 , however, one may obtain checkerboard-free or mesh-independent designs. Duysinx proposed to use an additional inner loop for efficient perimeter approximation (Duysinx, 1997). Beckers also applied the perimeter-control to the discrete design variable problems (Beckers, 1999).

2.2 Slope-constraint

The basic idea of the slope-constraint method is to constrain the gradient of design variables locally. In the work of Petersson and Sigmund (1998), the following additional constraints (for a two-dimensional case) are considered in optimization problems:

$$|\rho_{j+1,k} - \rho_{j,k}| \leq ch, \quad j=1, 2, \dots, n_x-1, k=1, 2, \dots, n_y \quad (11)$$

$$|\rho_{j+1,k} - \rho_{j,k}| \leq ch, \quad j=1, 2, \dots, n_x, k=1, 2, \dots, n_y-1 \quad (12)$$

In Eqs. (11) and (12), j and k denote the indices for the horizontal and the vertical locations of the design variable in the design domain discretized by $n_x \times n_y$ finite elements. The finite element size and the upper bound of the slope of a design variable are denoted by h and c , respectively. As shown in Eqs. (11) and (12), the number of additional constraints is approximately $2N_e (=2n_x \times n_y)$ for two-dimensional cases. Since

the additional constraints are linear, slope-constrained topology optimization problems can be solved efficiently by sequential linear programming. Like the perimeter-control, the slope-constraint can yield checkerboard-free and mesh-independent designs. Zhou et al. (2001) proposed an efficient algorithm that converts the constraints Eqs. (11) and (12) into adaptive side constraints requiring negligible computational efforts.

In comparison with filtering methods that will be discussed below, it is worth mentioning that both the perimeter-control and the slope-constraint are based on the same procedure in that the density differences are measured across finite element interfaces. The number of the additional constraints introduced by Eqs. (11) and (12) is the same as K in Eq. (9).

2.3 Filtering method

To suppress the checkerboard formation in the pressure distribution of Stoke's flow problems, Kikuchi et al. (1984) proposed to use 2×2 block basis functions which serve to filter out unwanted checkerboards. Later, Sigmund (1994) proposed a filtering method for topology optimization. He proposed two filters, that is a checkerboard-free filter and a mesh-independence filter which are similar to image filters. In the present work, we review the mesh-independence filter since it can cover the role of the checkerboard-free filter.

The mesh-independence filter may be expressed as:

$$\left(\rho_k \frac{\partial f}{\partial \rho_k} \right)^* = \frac{1}{\sum_{i=1}^{N_m} H_i} \sum_{i=1}^{N_m} H_i \left(\rho_i \frac{\partial f}{\partial \rho_i} \right) \quad (13)$$

$$H_i = r_m - \text{dist}(k, i), \quad \text{with } \text{dist}(k, i) \leq r_m \quad (14)$$

The weighted sensitivity $\rho_k \partial f / \partial \rho_k$ of the k th finite element is modified to $(\rho_k \partial f / \partial \rho_k)^*$ which is a weighted sum of the sensitivities of neighboring elements lying within a radius r_m of a mesh-independence filter. In Eq. (14), $\text{dist}(k, i)$ denotes the distance between the center of the k th and the i th element. Rewriting Eq. (13), one can define a transformation $T_{r_m}^m$ to express the filtered design sensitivity $(\partial f / \partial \rho_k)^*$ as:

$$\left(\frac{\partial f}{\partial \rho_k}\right)^* = T_{r_m}^m \left(\frac{\partial f}{\partial \rho_k}\right) = \frac{1}{\rho_k \sum_{i=1}^{N_m} H_i} \sum_{i=1}^{N_m} H_i \left(\rho_i \frac{\partial f}{\partial \rho_i}\right) \quad (15)$$

It can be easily seen that the original values of design sensitivities become unaltered when r_m goes to zero. An attractive aspect of this filtering scheme is that almost the same results as those by the perimeter-control and the slope-constraint method can be obtained without requiring much computational complexity.

3. Member-Sizing Filter

3.1 Relative evaluation of structural responses

The mesh-independence filter passes, for any value of r_m , only low-frequency image components in the current design sensitivity distribution. From a structural point of view, this filter serves to eliminate small-size structural components which may be obtained when a finer finite element mesh is employed. In many structural applications, robust designs avoiding too small-size members are desirable, for which the mesh-independence filtering technique (Sigmund, 1994) and the multi-scale multi-resolution strategy (Kim and Yoon, 2000) can be used. There are some situations when the sizes of structural components are limited by manufacturability, and thus small-size structural components are preferred. In this case, another technique may be needed. Extending the idea presented in Jeong et al. (2001), we propose a simple and efficient filter controlling structure member size.

The key idea of the present member-sizing filter is to select the high frequency components of a given design sensitivity field. Motivating by this idea, we propose the following form of a member-sizing filter:

$$\left(\rho_k \frac{\partial f}{\partial \rho_k}\right)^* = \frac{\rho_k \frac{\partial f}{\partial \rho_k}}{\frac{1}{N} \sum_{i=1}^{N_s} \rho_i \frac{\partial f}{\partial \rho_i}} = \frac{N_s}{\sum_{i=1}^{N_s} \rho_i \frac{\partial f}{\partial \rho_i}} \left(\rho_k \frac{\partial f}{\partial \rho_k}\right), \quad (16)$$

with $\text{dist}(k, i) \leq r_s$

The weighted design sensitivity $\rho_k(\partial f/\partial \rho_k)$ of the k th finite element is reevaluated relatively to

the average value of the neighboring sensitivities lying within a radius r_s .

We note that the original value of design sensitivities are recovered as r_s goes to infinity. Obviously, a small value of r_s will reduce the size of structural members of an optimized structure. Rewriting Eq. (16), one can define transformation $T_{r_s}^s$ acting on $\partial f/\partial \rho_k$, by which the size of structural members can be controlled. Since the transform $T_{r_s}^s$ requires almost the same operation as $T_{r_m}^m$, the additional computational complexity $T_{r_s}^s$ is marginal:

$$\left(\frac{\partial f}{\partial \rho_k}\right)^* = T_{r_s}^s \left(\frac{\partial f}{\partial \rho_k}\right) = \frac{N_s}{\sum_{i=1}^{N_s} \rho_i} \frac{\partial f}{\partial \rho_i} \quad (17)$$

In the application of the present member-sizing filter, the mesh-independence filter and the member-sizing filter are successively applied at every design iteration. It is worth noting that different member sizes can be obtained by the present filter even in a fixed finite element mesh. Since the topological complexity of an optimized structure is directly influenced by the member size, the present member-sizing filter may be viewed as a topology complexity controlling filter.

3.2 Application to the optimality criteria method

Using the Lagrangian function L , the optimality condition of the problem defined in Eqs. (1) ~ (3) is stated as

$$L(\boldsymbol{\rho}, \mu) = f(\boldsymbol{\rho}) + \mu g(\boldsymbol{\rho}) \quad (18)$$

$$\frac{\partial L}{\partial \rho_i} = \frac{\partial f}{\partial \rho_i} + \mu \frac{\partial g}{\partial \rho_i} = 0 \quad (19)$$

$$\frac{\partial L}{\partial \mu} = g = 0 \quad (20)$$

where μ is the Lagrange multiplier. By introducing the optimality index Π_i , Eq. (19) can be rewritten as:

$$\Pi_i(\rho_i, \mu) = -\left(\frac{\partial f}{\partial \rho_i} / \mu \frac{\partial g}{\partial \rho_i}\right) = 1 \quad (21)$$

From the optimality conditions expressed as Eqs. (20) and (21), the updating rule of the optimality

criteria method (Ma et al., 1993) is written as

$$\rho_i^{(m+1)} = \prod^\eta (\rho_i^{(m)}, \mu^{(m+1)}) \rho_i^{(m)} \quad (22)$$

$$\text{such that } g(\rho_i^{(m+1)}) = 0 \quad (23)$$

where m is the iteration number and η is the damping factor to control the convergence speed. In order to stabilize the updating procedure, proper move limits on the design variables should be applied.

It is well known that the procedure mentioned above is valid only if all of the design sensitivities $\partial f / \partial \rho_i$ of the objective function have negative signs. For some cases such as vibration problems, however, the design sensitivities $\partial f / \partial \rho_i$ may have both positive and negative signs. In these cases, the optimality criteria method needs to be modified by shifting the design sensitivities (Ma et al., 1993).

The member-sizing filter described in Eq. (17) requires that the signs of all the weighted design sensitivities $\rho_i(\partial f / \partial \rho_i)$ be the same. If the weighted design sensitivities have both positive and negative signs, the denominator in Eq. (17) may be vanishingly small. If this is the case, the weighted sensitivities $(\partial f / \partial \rho_i)^*$ may be unstable.

In order to satisfy the requirements invoked by the optimality criteria and the present member-sizing filter, the weighted design sensitivities are

shifted such that all the sensitivities become negative. Thus we modify the Lagrangian function of Eq. (18) as follows.

$$L(\boldsymbol{\rho}, \mu) = (f(\boldsymbol{\rho}) - \sigma g(\boldsymbol{\rho})) + (\mu + \sigma) g(\boldsymbol{\rho}) \quad (24)$$

$$= \bar{f}(\boldsymbol{\rho}) + \bar{\mu} g(\boldsymbol{\rho})$$

$$\sigma \geq \frac{\rho_i(\partial f / \partial \rho_i)}{\rho_i(\partial g / \partial \rho_i)} = \frac{\partial f / \partial \rho_i}{\partial g / \partial \rho_i}, \quad i = 1, 2, \dots, N_e \quad (25)$$

where \bar{f} and $\bar{\mu}$ denote the modified objective function and the corresponding new Lagrange multiplier. As can be seen from Eqs. (24) and (25), both the design sensitivities $\partial \bar{f} / \partial \rho_i$ and weighted design sensitivities $\rho_i(\partial \bar{f} / \partial \rho_i)^*$ of the modified objective function are always negative. The overall procedure of the present scheme is depicted in Fig. 1.

4. Numerical Examples

4.1 Static compliance minimization of the MBB beam

As the first example, the MBB (Messerschmitt-Bolkow-Blohm) beam design problem is considered. Fig. 2 illustrates the problem definition. The applied force and material properties are $F = 200,000$ and $E = 2.0 \times 10^8$, $\nu = 0.3$, respectively. The design target is to minimize the mean compliance subject to a 30% mass constraint.

As mentioned in section 2, the mesh-independence filter may be used as a checkerboard-free filter. In the present work, we use $r_m = 1.1h$ for the mesh-independence filter in order to suppress the formation of checkerboard patterns. This filtering may be denoted by the transform $T_{1.1h}^m$.

More complex structures may be obtained as the finite element mesh gets finer. However, no drastic change has occurred as shown in Fig. 3 (For the results in Fig. 3, only the checkerboard-

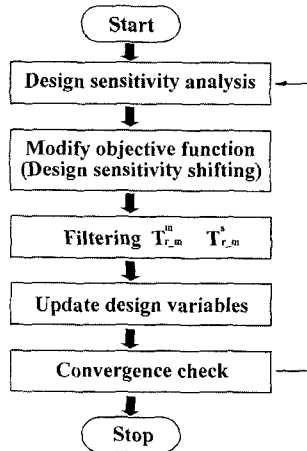


Fig.1 Topology optimization procedure using filters (mesh-independence or checkerboard-free filter $T_{r_m}^m$, member-sizing filter $T_{r_s}^s$)

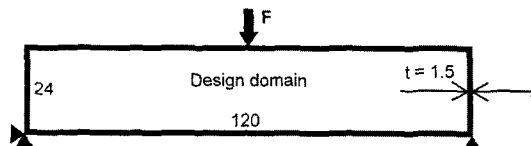


Fig. 2 Initial design domain of the MBB beam

free filter is employed.). Since the mesh-independence and/or the checkerboard-free filtering smears out the high-frequency components of an image, the relative dominance of design sensitivities in a local area cannot be emphasized. Since the present member-sizing filter emphasizes the local dominance of member, however, small-size members can be obtained.

The results obtained after the application of the present member-sizing filter are shown in Fig. 4. Since the member-sizing filter is based on the concept opposite to the checkerboard-free filter, the application of the member-sizing filter alone results in severe checkerboard patterns, as illustrated in Fig. 4(a). Thus we incorporate the checkerboard filtering scheme into the member-sizing filter as:

$$\left(\frac{\partial f}{\partial \rho_i}\right)^* = T_{r_s}^s \circ T_{1.1h}^m \left(\frac{\partial f}{\partial \rho_i}\right) = T_{r_s}^s \left(T_{1.1h}^m \left(\frac{\partial f}{\partial \rho_i}\right)\right) \quad (26)$$

$$\left(\frac{\partial f}{\partial \rho_i}\right)^* = T_{1.1h}^m \circ T_{r_s}^s \left(\frac{\partial f}{\partial \rho_i}\right) = T_{1.1h}^m \left(T_{r_s}^s \left(\frac{\partial f}{\partial \rho_i}\right)\right) \quad (27)$$

Figures 4 (b) and 4 (c) show the effects of the composed filters defined in Eqs. (26) and (27),



(a) Using the member-sizing filter ($T_{r_s}^s$) alone



(b) Using the checkerboard-free filter followed by the member-sizing filter ($T_{r_s}^s \circ T_{1.1h}^m$)



(c) Using the member-sizing filter followed by the checkerboard-free filter ($T_{1.1h}^m \circ T_{r_s}^s$)

Fig. 4 Results of the MBB beam design with $r_s=6.0$ (mesh : 48×240)



(a) 16×80 mesh ($h=2.2$)



(b) 32×160 mesh ($h=1.0$)



(c) 48×240 mesh ($h=0.5$)



(d) 64×320 mesh ($h=0.25$)



(e) 128×640 mesh ($h=0.125$)

Fig. 3 Results of the MBB beam design problem with the varying element size h



(a) $r_s = \infty$ (No filtering)



(b) $r_s = 12.0$



(c) $r_s = 6.0$



(d) $r_s = 3.0$



(e) $r_s = 1.5$

Fig. 5 Results of the MBB beam design with the varying value of r_s (48×240 mesh, $T_{r_s}^s \circ T_{1.1h}^m$)

Table 1 The values of the objective function for varying values of radius r_s of the member-sizing filter

r_s	Objective function (Mean compliance)
∞ (No filtering)	35876
12.0	35131
6.0	36763
3.0	39366
1.5	47759

respectively. We use $r_s=6.0$ to obtain the results shown in Fig. 4. Regardless of the application order of the two filters, almost the same results, having no checkerboard, are obtained. Comparing the results in Figs. 4 (b) and 4(c) with that in Fig. 3(c), one can see that more complex structures are obtained when a member-sizing filter ($r_s < \infty$) is applied.

In Fig. 5, the effects of the radius r_s of the member-sizing filter are investigated. It is clear that the structural member size is controlled by the value of r_s . The objective function values are listed in Table 1 for different values of the radius r_s . Table 1 shows that the value of the objective function increases as the value of r_s decreases. Obviously, this is because any filtering method restricts the design space and the lower value of r_s restricts the space tighter. However, the reduction in the objective function value can be compensated by the achievement of the structural member of a desired size.

4.2 Multiple eigenfrequency maximization of a two-dimensional beam

In this case study, the reinforcement of a two-dimensional beam to maximize eigenfrequencies is dealt with. The design objective is to maximize the first four eigenfrequencies. The design problem is subject to a 30% mass constraint. The initial design domain is shown in Fig. 6(a) and its first four eigenmodes are plotted in Fig. 6(b). The third eigenmode in Fig. 6(b) is a local mode. To find the initial eigenmodes shown in Fig. 6, the uniform density of $\rho=0.3$ is used for all the elements in the design domain. Each point mass

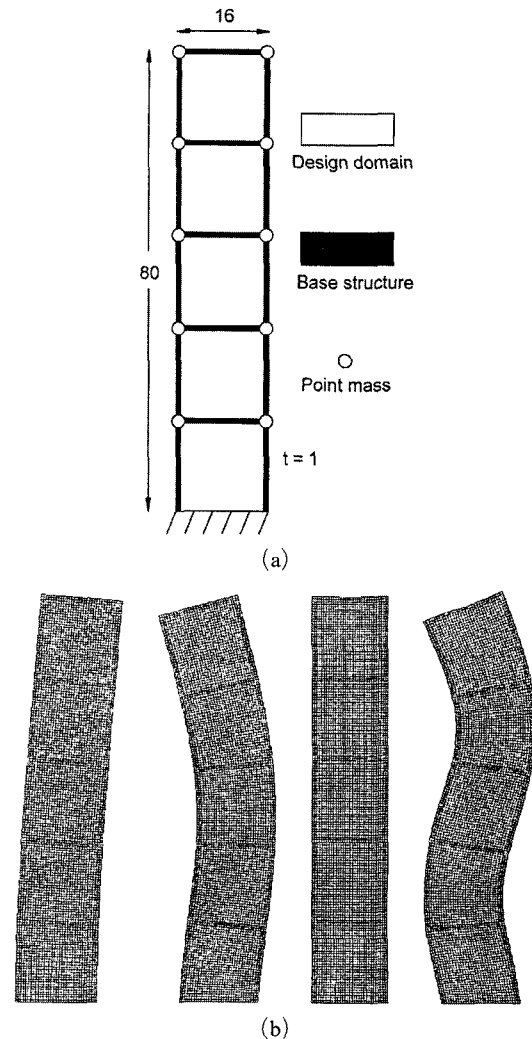


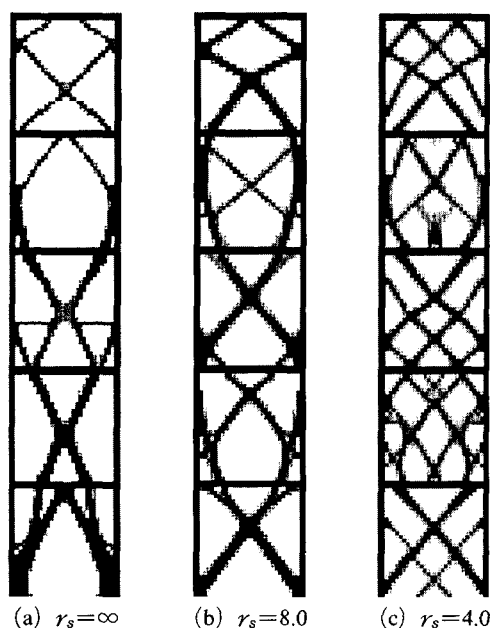
Fig. 6 (a) Initial design domain of a two-dimensional beam and (b) Its first four eigenmodes (160×32 mesh, element size $h=0.5$)

at ten locations shown in Fig. 6(a) weights 20.0, and material properties used for the design domain are $E=2.0 \times 10^8$, $\nu=0.3$. The function defined in Eq. (5) with $w_1=\dots=w_4=1.0$ is used as the objective function.

Fig. 7 shows the results obtained with different values of r_s . As in the compliance minimization problem, the member size becomes smaller as the value of r_s becomes smaller. The eigenfrequencies obtained with different values of r_s are given in Table 2. It is remarked that the improvement in the lower eigenfrequencies is not so significant

Table 2 Eigenfrequency changes with varying r_s

	Initial value	$r_s=\infty$ (No filtering)	$r_s=8.0$	$r_s=4.0$
1st eigenfrequency (Hz)	3.46	4.37 (+26.3%)	4.04 (+16.76%)	3.94 (+13.87%)
2nd eigenfrequency (Hz)	12.88	17.78 (+38.0%)	19.16 (+48.76%)	18.41 (+42.93%)
3rd eigenfrequency (Hz)	21.88	28.28 (+29.3%)	25.10 (+14.71%)	23.10 (+5.58%)
4th eigenfrequency (Hz)	26.01	34.98 (+34.5%)	46.14 (+77.39%)	44.28 (+70.24%)

**Fig. 7** Optimal reinforcement of a two-dimensional beam with respect to its first four eigenfrequencies

as r_s becomes smaller. On the other hand, the improvement in the third and fourth eigenfrequencies is noticeable as r_s becomes smaller. Again, it is clear that the present member-sizing filter can control the member size of an optimized structure successfully.

5. Conclusions

In this paper, a new filter to control the member size of an optimized structure has been proposed. The present member-sizing filter reevaluates the

sensitivity relatively to the average sensitivity within a prescribed radius of the member-sizing filter. Several numerical examples have confirmed that the member size can be effectively controlled by the proposed filter; the smaller the filter radius is, the finer the member size becomes. Due to marginal computational efforts required in the present filtering process, the present technique can be effective even for large-scale industrial design problems. The member-sizing filter developed in this work is expected to play some roles in the design of buildings and civil structures where aesthetics is also a very important issue.

Acknowledgment

Numerical work was performed on the Alpha-11 cluster at SAIT (Samsung Advanced Institute of Technology).

References

- Beckers, M., 1999, "Topology Optimization Using a Dual Method with Discrete Variables," *Structural Optimization*, Vol. 17, pp. 12~24.
- Bendsøe, M. P. and Sigmund, O., 2003, *Topology Optimization; Theory, Methods and Applications*, Springer-Verlag Berlin Heidelberg.
- Bourdin, B., 2001, "Filters in Topology Optimization," *International Journal for Numerical Methods in Engineering*, Vol. 50, pp. 2143~2158.
- Duysinx, P., 1997, "Layout Optimization: A Mathematical Programming Approach," *DCA-MM Report*, No. 540, Technical University of

Denmark.

Haber, R. B., Jog, C. S. and Bendsøe, M. P., 1996, "A New Approach to Variable-Topology Shape Design Using a Constraint on Perimeter," *Structural Optimization*, Vol. 11, pp. 1~12.

Jeong, J. H., Kim, T. S. and Kim, Y. Y., 2001, "A New Grain-Sizing Filter in Topology Optimization," *Extended Abstracts of the Fourth World Congress of Structural and Multidisciplinary Optimization*, pp. 46~47.

Kikuchi, N., Oden, J. T. and Song, Y. J., 1984, "Convergence of Modified Penalty Methods and Smoothing Schemes of Pressure for Stoke's flow Problems," *Finite elements in Fluids*, Vol. 5, pp. 107~126.

Kim, T. S. and Kim, Y. Y., 2002, "Multi-Objective Topology Optimization of a Beam Under Torsion and Distortion," *AIAA Journal*, Vol. 40 (2), pp. 376~381.

Kim, Y. Y. and Yoon, G. H., 2000, "Multi-Resolution Multi-Scale Topology Optimization—A New Paradigm," *International Journal of Solids and Structures*, Vol. 37, pp. 5529~5559.

Ma, Z. D., Kikuchi, N. and Hagiwara, I., 1993, "Structural Topology and Shape Optimization for a Frequency Response Problem," *Computational*

Mechanics, Vol. 13, pp. 157~174.

Ma, Z. D., Kikuchi, N. and Cheng, H. C., 1995, "Topological Design for Vibrating Structures," *Computer Methods in Applied Mechanics and Engineering*, Vol. 121, pp. 259~280.

Park, S. H. and Youn, S. K., 1997, "A Study on the Topology Optimization of Structures," *KSME Journal*, Vol. 21 (8), pp. 1241~1249. (In Korean)

Petersson, J. and Sigmund, O., 1998, "Slope Constrained Topology Optimization," *International Journal for Numerical Methods in Engineering*, Vol. 41, pp. 1417~1434.

Sigmund, O., 1994, *Design of Material Structures Using Topology Optimization*. Ph. D. Thesis, Department of Solid Mechanics, Technical University of Denmark.

Youn, S. K. and Park, S. H., 1997, "A Study on the Shape Extraction in the Structural Topology Optimization Using Homogenized Material," *Computers & Structures*, Vol. 62 (3), pp. 527~538.

Zhou, M., Shyy, Y. K. and Thomas, H. L., 2001, "Checkerboard and Minimum Member Size Control in Topology Optimization," *Structural Optimization*, Vol. 21, pp. 152~158.